© 2015. Published by The Company of Biologists Ltd | Journal of Cell Science (2015) 128, 1982-1990 doi:10.1242/jcs.167858

RESEARCH ARTICLE

GSTO1-1 modulates metabolism in macrophages activated through the LPS and TLR4 pathway

Deepthi Menon[1], Rebecca Coll[2], Luke A. J. O'Neill[3] and Philip G. Board[1,*]

ABSTRACT

Macrophages mediate innate immune responses that recognise foreign pathogens, and bacterial lipopolysaccharide (LPS) recruits a signalling pathway through Toll-like receptor 4 (TLR4) to induce pro-inflammatory cytokines and reactive oxygen species (ROS). LPS activation also skews the metabolism of macrophages towards a glycolytic phenotype. Here, we demonstrate that the LPS-triggered glycolytic switch is significantly attenuated in macrophages deficient for glutathione transferase omega-1 (GSTO1, note that GSTO1-1 refers to the dimeric molecule with identical type 1 subunits). In response to LPS, GSTO1-1-deficient macrophages do not produce excess lactate, or dephosphorylate AMPK, a key metabolic stress regulator. In addition, GSTO1-1-deficient cells do not induce HIF1α, which plays a key role in maintaining the pro-inflammatory state of activated macrophages. The accumulation of the TCA cycle intermediates succinate and fumarate that occurs in LPS-treated macrophages was also blocked in GSTO1-1-deficient cells. These data indicate that GSTO1-1 is required for LPS-mediated signalling in macrophages and that it acts early in the LPS–TLR4 pro-inflammatory pathway.

KEY WORDS: Metabolism, GSTO1-1, TLR4, Redox, LPS

INTRODUCTION

Innate immunity is considered as the first line of defence against invading pathogens in mammals. The activation of macrophages resulting from the interaction of the bacterial cell wall component lipopolysaccharide (LPS) with Toll-like receptor 4 (TLR4) constitutes a major pathway for the initiation of innate immune responses and the development of inflammation. In macrophages, activation of TLR4 by LPS has been shown to recruit downstream signalling proteins and induce the generation of reactive oxygen species (ROS) and pro-inflammatory cytokines such as interleukin (IL)-1β, IL-6 and TNFα (Doyle and O'Neill, 2006; Gill et al., 2010; Stoll et al., 2006; Zhang and Ghosh, 2001; Zhou et al., 2010). In addition to their bactericidal activity, their signalling role and their impact on the expression of pro-inflammatory cytokines, the ROS generated by the TLR4 pathway have also been shown to cause tissue damage and are central to the progression and pathology of many inflammatory diseases (Gill et al., 2010).

We have previously shown that Omega class glutathione transferase-1 (GSTO1, note that GSTO1-1 refers to the dimeric molecule with identical type 1 subunits) is essential for the generation of cytosolic ROS after the activation of the TLR4 pro-inflammatory cascade (Menon et al., 2014). GSTO1-1-deficient macrophages are non-responsive to LPS and do not activate nuclear factor (NF)-κB and NADPH oxidase 1 after TLR4 activation. Since their first description, the Omega class GSTs have been investigated in relation to a number of biologically significant pathways and clinical disorders including drug resistance, Alzheimer's disease, Parkinson's disease, vascular dementia and stroke, amyotrophic lateral sclerosis, the action of anti-inflammatory drugs, the disposition of arsenic, susceptibility to chronic obstructive pulmonary disease (COPD) and cancer (Allen et al., 2012; Escobar-Garcia et al., 2012; Harju et al., 2007; Kölsch et al., 2004; Li et al., 2003; Piacentini et al., 2012). Because inflammation has been implicated in the pathology associated with many of these disorders it is important to understand the mechanism by which GSTO1-1 mediates inflammatory responses in macrophages. Here, we have investigated the role of GSTO1-1 in the activation of parallel pathways that generate mitochondrial ROS and indirectly feed into TLR4 signalling. In light of recent studies showing that TLR4 activation by LPS skews macrophage metabolism towards a more glycolytic phenotype (Freemerman et al., 2014; Haschemi et al., 2012; Tannahill et al., 2013), we examined the metabolic profile of GSTO1-1-deficient macrophages. We found that GSTO1-1 plays a key role in determining the glycolytic phenotype of LPS-activated macrophages and also dictates the redox processes in macrophages necessary to mediate inflammatory responses.

RESULTS

GSTO1-1 mediates pro-inflammatory responses in macrophages

LPS has previously been shown to increase mitochondrial ROS generation and contribute to the pro-inflammatory response in macrophages (Mo et al., 2014; Poltorak et al., 1998; Thimmulappa et al., 2006). We confirmed this finding and measured a significant (P=0.05) increase in mitochondrial ROS in LPS-treated J774.1A non-silencing control cells. This response was absent in GSTO1-knockdown cells (Fig. 1A), suggesting that GSTO1-1 is required for mitochondrial ROS production in addition to its previously demonstrated effect on cytosolic ROS (Menon et al., 2014). As a consequence of the oxidative stress resulting from the increased cytosolic and mitochondrial ROS, we found that there was a significant decrease in the GSH:GSSG ratio of LPS-treated control J774.1A cells (Fig. 1B). In comparison there was no change in the GSH:GSSG ratio in GSTO1-knockdown cells treated with LPS. This is consistent with the lack of ROS production in these cells.

In subsequent studies, we evaluated changes in the transcript levels of inflammatory markers that are influenced by oxidative stress in macrophages. An increase in ROS levels and/or a decrease in antioxidants such as glutathione have both previously been demonstrated to induce the expression of cyclooxygenase-2 (COX-2, also known as PTGS2) and inducible nitric oxide synthase (iNOS,

[1]Department of Molecular Biosciences, John Curtin School of Medical Research, Australian National University, Canberra, ACT 2600, Australia. [2]Institute for Molecular Bioscience, The University of Queensland, St Lucia 4072, Australia. [3]School of Biochemistry and Immunology, Trinity Biomedical Sciences Institute, Trinity College Dublin, Dublin 2, Ireland.

*Author for correspondence (Philip.Board@anu.edu.au)

Received 17 December 2014; Accepted 10 March 2015

Journal of Cell Science

Journal of Cell Science (2015) 128, 1982-1990 doi:10.1242/jcs.167858

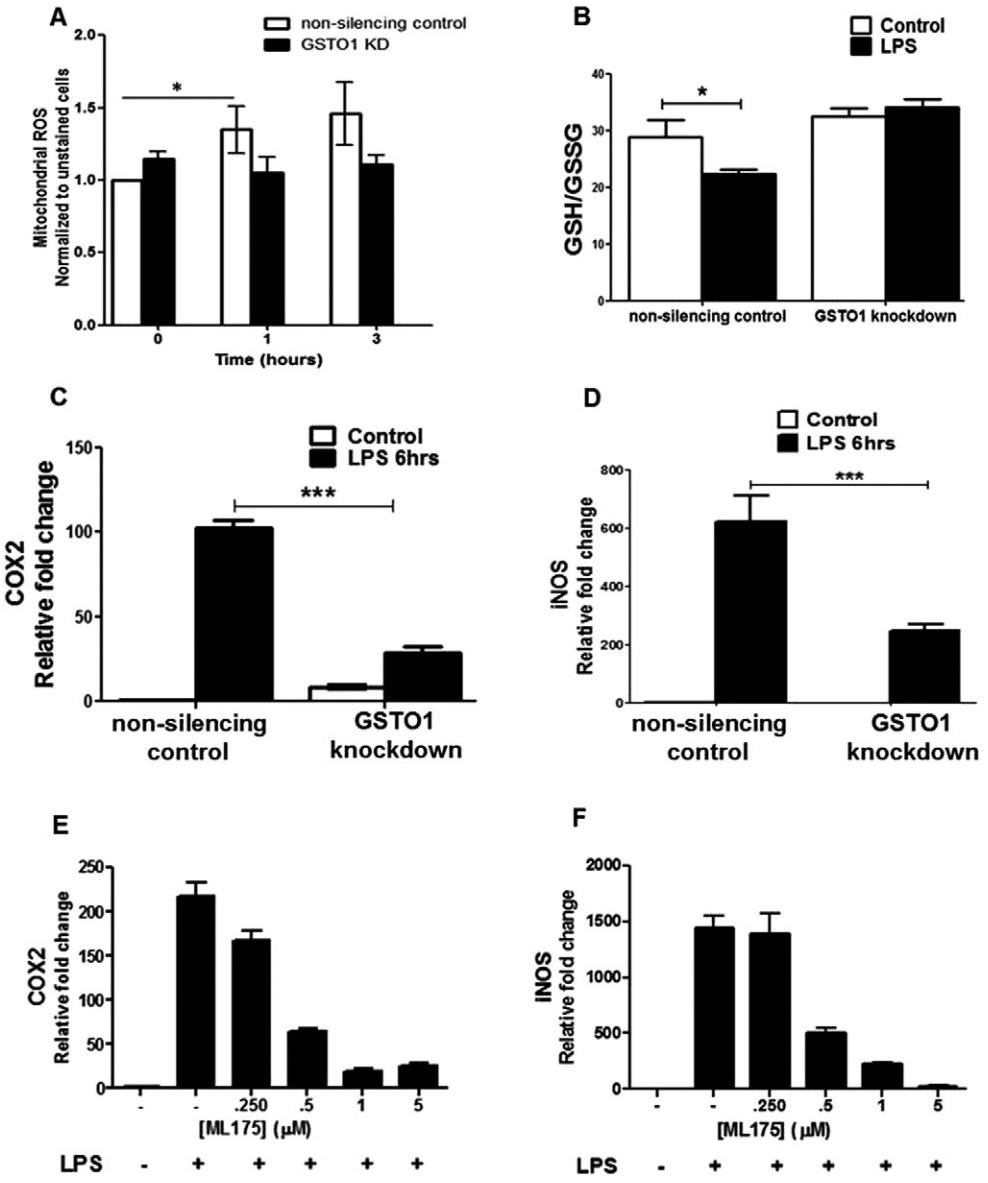

Fig. 1. GSTO1-1 mediates pro-inflammatory responses in LPS-activated macrophages. (A) LPS-treated non-silencing control cells showed a significant (*P=0.05) increase in mitochondrial ROS which was absent in the GSTO1-knockdown (GSTO1 KD) cells. (B) As a consequence of increased oxidative stress resulting from the increased cytosolic and mitochondrial ROS, a significant (*P<0.05) drop in the GSH:GSSG ratio was measured in the non-silencing control cells. The J774.1A GSTO1-knockdown cells showed no alteration in the GSH:GSSG ratio, suggesting an overall absence of oxidative stress in these cells. (C–F) Fold changes in mRNA. (C,D) LPS-treated macrophages deficient in GSTO1-1 showed a significantly (***P<0.001) reduced induction of redox-sensitive pro-inflammatory markers, such as COX2 (C) and iNOS (D). (E,F) The induction of COX2 and iNOS was abolished in LPS-activated macrophages pre-treated with ML175, mimicking GSTO1-knockdown cells and suggesting the catalytic involvement of GSTO1-1 in LPS signalling. All data are shown as the mean±s.e.m. (n=3).

also known as NOS2) in LPS-treated macrophages (D'Acquisto et al., 1997; Raso et al., 2001; Wadleigh et al., 2000). The induction of COX-2 and iNOS after LPS treatment was significantly diminished in GSTO1-1-deficient macrophages (Fig. 1C,D). This lack of response is possibly due to the lack of stimuli in the form of increased ROS or decreased GSH (Chen et al., 1999). Similarly, when LPS-activated non-silencing control J774.1A macrophages were pre-treated with ML175, to inhibit GSTO1-1, the induction of COX2 and iNOS was significantly attenuated (Fig. 1E,F). This result strongly suggests that the action of GSTO1-1 on LPS-initiated inflammation is dependent on its catalytic activity.

Mitochondrial dysfunction in LPS stimulated macrophages is abrogated in GSTO1 knockdown cells

In addition to its effect on mitochondrial ROS production, we also examined the effect of GSTO1-1 on the previously noted decrease in mitochondrial membrane potential (ψ) that occurs after LPS stimulation (Mo et al., 2014). We detected a significant (P<0.05) decrease in the mitochondrial membrane potential in LPS treated J774.1A non-silencing control cells. In contrast, LPS did not significantly change the mitochondrial membrane potential of GSTO1-1-deficient cells (Fig. 2A).

It has been previously established that an altered mitochondrial membrane potential is associated with an imbalance in the AMP:ATP ratio that is monitored by AMP-activated protein kinase (AMPK), a major sensor of intracellular energy status (Mo et al., 2014). As recent evidence suggests that there is a substantial link between energy homeostasis and redox state in macrophages (Gauss et al., 2007; Maitra et al., 2009; Matsuzawa et al., 2005; Meissner et al., 2008; Menon et al., 2014; Mo et al., 2014; West et al., 2011), we further investigated the role of GSTO1-1 in modulating the LPS-stimulated decrease in the mitochondrial membrane potential by evaluating the amount of phosphorylated AMPK (p-AMPK), which is indicative of the amount of activated AMPK. The results indicate that the activation of AMPK to p-AMPK is diminished by a pro-inflammatory stimulus such as LPS, and this effect is dependent on GSTO1-1, given that normal levels of p-AMPK remained in GSTO1-knockdown cells after

Journal of Cell Science (2015) 128, 1982-1990 doi:10.1242/jcs.167858

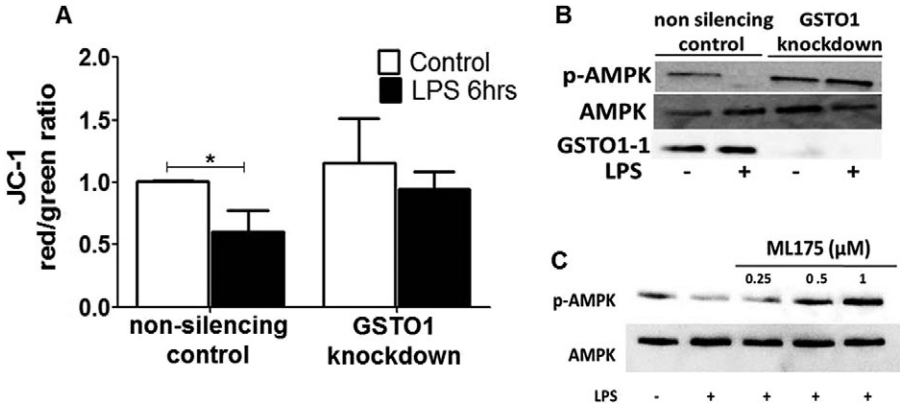

Fig. 2. GSTO1-1 modulates mitochondrial function and energy status in LPS-treated macrophages. (A) The significant (*P<0.05) decrease in the mitochondrial membrane potential (ψ) in LPS-treated J774.1A non-silencing control cells was absent in the GSTO1-1-deficient cells. (B) The inhibitory effect of LPS on AMPK phosphorylation in J774.1A macrophages is reversed in GSTO1-1-deficient cells. (C) AMPK activation was restored by ML175 in LPS-activated macrophages. All data are shown as the mean±s.e.m. (n=3).

LPS stimulation (Fig. 2B). To further determine whether the LPS-triggered loss of p-AMPK is dependent on the catalytic activity of GSTO1-1, we tested the ability of ML175 to maintain normal p-AMPK levels. As shown in Fig. 2C, AMPK phosphorylation was restored by ML175 treatment in a concentration-dependent manner.

Reconfiguration of cellular metabolism during pro-inflammatory polarization of M1 macrophages

The observed requirement for GSTO1-1 in the maintenance of the normal mitochondrial response to LPS in macrophages and in the activation of AMPK suggested that GSTO1-1 is also be required for the well-documented shift in macrophage metabolism towards glycolysis after LPS activation (Freemerman et al., 2014; Haschemi et al., 2012; Tannahill et al., 2013).

We therefore compared the extracellular acidification rate (ECAR) and oxygen consumption rate (OCR) of LPS-activated GSTO1 knockdown and control macrophages. As shown in Fig. 3A,B, a steady increase in the ECAR (reflecting increased glycolysis) in control cells treated with LPS was blocked in GSTO1-knockdown cells. In contrast, OCR levels (reflecting oxidative phosphorylation) inversely mirrored ECAR changes in control cells. The OCR showed a steady decline in control cells and there was no change in GSTO1-deficient macrophages (Fig. 3B). To complement the ECAR measurements in GSTO1-deficient cells, we quantified the lactate secreted into the medium by the cells after LPS stimulation. As expected, we measured a significant increase (P<0.001) in the extracellular lactate levels in cells expressing non-silencing control, confirming the shift in their metabolism away from mitochondrial oxidative phosphorylation to glycolysis. However, the GSTO1-knockdown cells did not alter their lactate secretion, confirming that the cells did not respond to LPS and acquire a glycolytic phenotype (Fig. 3C). Consistent with the requirement for GSTO1-1 in the LPS-induced glycolytic shift, we also found that the inhibitor ML175 caused a concentration-dependent decrease in lactate production by J774.1A cells after LPS treatment (Fig. 3D).

In addition to increased glycolysis through the Emden–Meyerhof pathway, increased flux through the pentose phosphate pathway (PPP) can also contribute to lactate production. Increased flux through the PPP generates NADPH that is required by NADPH oxidases to generate high levels of ROS after TLR4 activation. We found that NADPH levels were significantly increased in LPS-stimulated non-silenced J774.1A macrophage-like cells, but no increase was observed in GSTO1-knockdown cells (Fig. 3E) or in cells treated with ML175 (Fig. 3F).

LPS-induced accumulation of succinate and the stabilization of HIF1α

The TCA cycle intermediate succinate is an inflammatory signal that increases in macrophages following stimulation with LPS and the subsequent metabolic shift (Tannahill et al., 2013). In metabolomics experiments performed after LPS activation of non-silenced J774.1A cells, we found the expected build-up of the Kreb's cycle intermediate succinate and a relatively lower accumulation of fumarate. This response was abolished in GSTO1-deficient cells, reflecting the absence of a glycolytic phenotype in these cells (Fig. 4A,B). In these studies, the abundance of TCA metabolites was normalized to the total number of cells and to the amount of essential amino acids (Leu, Ile or Met) detected in the cell lysates. Citrate levels also showed a similar trend in LPS-treated control macrophages but remained unaltered in GSTO1-1-deficient macrophages (Fig. 4C). Metabolomic profiling also identified that the levels of the glycolytic intermediates glucose 6-phosphate and fructose 6-phosphate were dependent on the expression of GSTO1-1 (Fig. 4D). This trend in sugar phosphates was previously reported in macrophages overexpressing carbohydrate kinase-like protein (CARKL, also known as SHPK) and was found to dampen the pro-inflammatory responses of TLR4-activated macrophages (Haschemi et al., 2012).

Previous studies have shown that the accumulation of succinate during the LPS-mediated activation of macrophages stabilizes the transcription factor HIF1α and promotes the transcription of IL-1β (Tannahill et al., 2013). We found that the accumulation of HIF1α normally triggered by LPS is blocked in GSTO1-1-deficient cells (Fig. 4E). This is consistent with the failure of GSTO1-1-deficient cells to accumulate succinate. In additional studies of HIF1α (Fig. 4F), we found that inhibition of GSTO1-1 with ML175 mimicked the effects of silencing GSTO1-1 in macrophages in a dose-dependent manner.

Modulating the metabolic profile of macrophages blocks the activation of the M1-macrophage-like phenotype

To evaluate the consequences of disrupted metabolism in GSTO1-1 deficient cells, we measured the phagocytic ability of the cells both qualitatively and quantitatively using two independent approaches in order to determine whether the cells behave like M1 macrophages upon LPS stimulation. J774.1A non-silencing control cells internalized fluorescently labelled dead bacteria efficiently indicating a collective response of all TLRs to the presence of pathogenic agents in the microenvironment. Further, J774.1A non silencing control cells primed with LPS for 2 h prior to incubation with the fluorescently labelled dead bacteria significantly enhanced phagocytosis (Fig. 5A). Interestingly, GSTO1-deficient cells showed poor efficacy in the

Journal of Cell Science (2015) 128, 1982-1990 doi:10.1242/jcs.167858

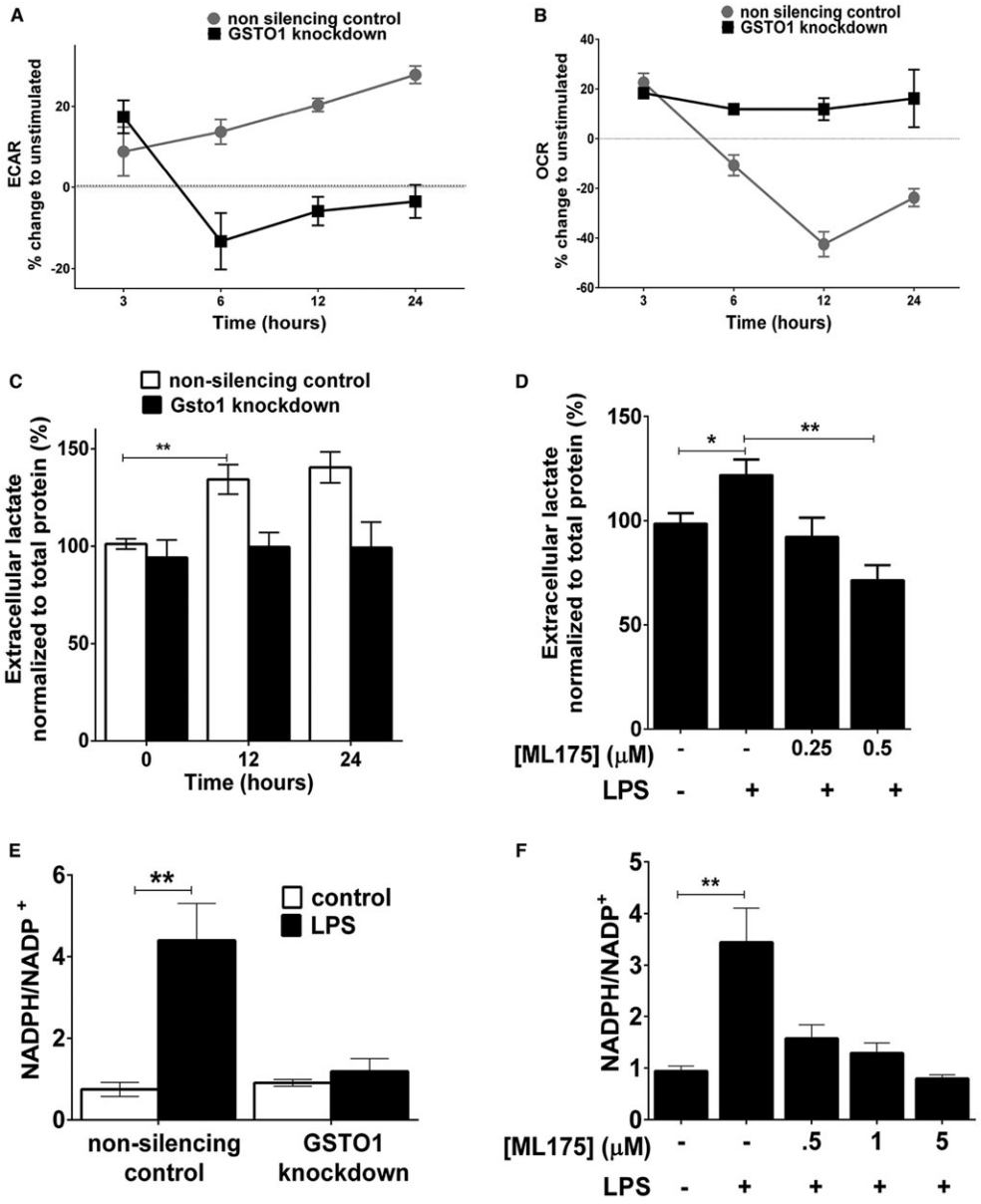

Fig. 3. GSTO1-1 deficiency blocks the development of a glycolytic phenotype in LPS-activated macrophages. (A) The LPS-induced increase in ECAR measured in non-silencing J774.1A macrophages was largely absent in the GSTO1-1-deficient macrophages. (B) The LPS-induced decrease in the OCR observed in non-silencing J774.1A macrophages did not occur in GSTO1-1 deficient macrophages. (C) Significantly (**P<0.01) increased extracellular lactate levels confirmed the high rate of LPS-induced extracellular acidification in control cells, whereas the level of extracellular lactate was unchanged in the supernatant from GSTO1-1-deficient cells treated with LPS. (D) Wild-type J774.1A macrophages treated with LPS showed a significant (*P<0.05) dose-dependent decrease in the extracellular lactate level when GSTO1-1 was inhibited with ML175. (E,F) NADPH levels were significantly (**P<0.01) increased in LPS-stimulated J744.1A non-silencing macrophage cells (E) but no increase was measured in the GSTO1-1-deficient cells and in cells treated with ML175 (F). All data are shown as the mean±s.e.m. (A,B, n=5; C–F, n=3).

internalization of the pathogenic particles and also remained unstimulated after priming with LPS (Fig. 5A). Cell viability was evaluated to eliminate any difference in the cell viability post bacterial exposure (Fig. 5B). To further narrow down the non-responsiveness of GSTO1-knockdown cells, latex beads coated with LPS were applied to the cells to specifically activate TLR4. We found that GSTO1-1-deficient cells failed to internalize the LPS-coated latex micro particles (in red) to the extent seen with the non-silenced control cells (Fig. 5C–E).

DISCUSSION

Previous studies have established that macrophages activated through the LPS–TLR4 pathway produce ROS and develop a glycolytic phenotype that is characterized by the increased production of lactate and the accumulation of succinate, which stabilizes HIF1α and regulates the expression of IL-1β. Recently, we demonstrated that GSTO1-1 is required for the activation of NF-κB and the production of cytosolic ROS in macrophages stimulated by LPS (Menon et al., 2014). In the present study, we have investigated the role of GSTO1-1 in the production of ROS during mitochondrial metabolism and the development of a glycolytic phenotype in LPS-activated macrophages. Our results show that GSTO1-1 is also required for the generation of mitochondrial ROS, which, taken together with our previous data, indicates that GSTO1-1 is a significant regulator of ROS production and a determinant of redox balance in LPS-activated macrophages. ROS are major mediators of cytotoxicity and are directly responsible for much of the pathology that is associated with inflammation. As inflammation contributes to the pathology and progression of a wide range of disorders this finding might explain the previously reported associations between genetic variations in *GSTO1* and Alzheimer's disease, Parkinson's disease, vascular dementia and stroke, amyotrophic lateral sclerosis and chronic obstructive pulmonary disease (COPD) (Allen et al., 2012; Escobar-Garcia et al., 2012; Harju et al., 2007; Kölsch et al., 2004; Li YJ et al., 2003; Piacentini et al., 2012). The investigation of GSTO1-1 in other disorders that are influenced by inflammation would appear to be warranted.

Our present data also indicates that GSTO1-1 is required for the major metabolic shift to a glycolytic phenotype that occurs in

Journal of Cell Science (2015) 128, 1982-1990 doi:10.1242/jcs.167858

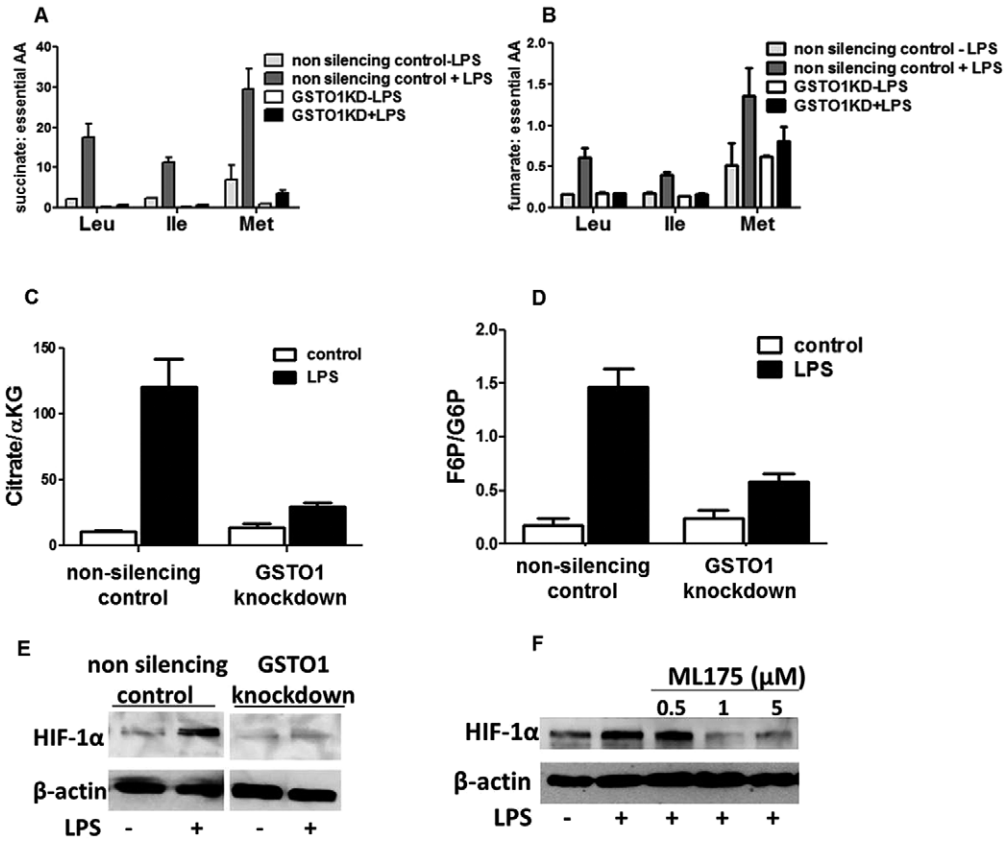

Fig. 4. LPS-dependent reprogramming of the TCA cycle in M1 macrophages is altered by GSTO1-1 knockdown. (A,B) The accumulation of succinate and fumarate intermediates in LPS-treated J774.1A non-silencing macrophages was substantially attenuated in GSTO1-1-deficient cells (GSTOIKD). Data was normalized to levels of Leu, Ile or Met. (C) Citrate levels also remained unchanged in LPS-treated GSTO1-knockdown macrophages. HIF1α is stabilized by LPS stimulation of macrophages. (D) The accumulation of F6P in LPS-stimulated J744 non-silencing control macrophages is attenuated in GSTO1-1-deficient cells. (E) The induction of HIF1α stimulated by LPS in J744 non-silencing macrophages is significantly attenuated in GSTO1-1-deficient cells. (F) Inhibition of GSTO1-1 catalytic activity with ML175 mimicked the effects of silencing GSTO1 in macrophages in a dose-dependent manner. All data are shown as the mean±s.e.m. (*n*=3).

LPS-activated macrophages. We found that GSTO1-1 deficiency blocks the increased production of lactate and the decrease in oxygen consumption that normally follows LPS stimulation. In addition, metabolomic studies showed that GSTO1-1 deficiency blocked the accumulation of succinate that has been shown to be a major inflammatory signal that stabilizes HIF1α allowing the subsequent induction of IL-1β. This finding was supported by the observation that HIF1α does not accumulate in GSTO1-1-deficient macrophages stimulated with LPS.

Taken together with our previous studies, the present data indicate that GSTO1-1 is required for the activation of macrophages by LPS and is a determinant of all the redox and metabolic changes that occur. The activation of macrophages by LPS occurs through several parallel pathways that include the activation of NF-κB, and the development of a glycolytic phenotype discussed above (Fig. 6A). Both these pathways promote the production of ROS and the expression of pro-inflammatory cytokines, such as IL-1β. The finding that GSTO1-1 deficiency blocks both activation pathways places the site of GSTO1-1 action upstream and possibly in the TLR4–myddosome complex (Fig. 6A).

These findings identify GSTO1-1 as a new anti-inflammatory target. Indeed, the treatment of LPS-stimulated J774.1A cells with the GSTO1-1 inhibitor ML175 blocked all the metabolic effects associated with macrophage activation including the generation of ROS, the induction of COX2 and iNOS, the accumulation of HIF1α, and the increase in lactate production through glycolysis. The observation that the effects of ML175 are dose dependent provides additional evidence that inflammation might be pharmacologically targeted through the development of novel GSTO1-1 inhibitors.

Given that a pharmacological inhibitor of GSTO1-1 was found to be effective in blocking LPS stimulated activation it seems likely that the regulatory effect of GSTO1-1 is mediated by its catalytic activity. Several studies (Anathy et al., 2012; Cooper et al., 2011; Dalle-Donne et al., 2009; Lim et al., 2010) have suggested that protein glutathionylation can provide a reversible switch that can regulate protein function and potentially regulate pathways in a manor analogous to protein phosphorylation. We have previously shown that GSTO1-1 can catalyse glutathionylation cycle reactions (Menon and Board, 2013) and in this study we found that total glutathionylation of proteins was significantly elevated in GSTO1-1-knockdown cells compared with wild-type and non-silencing control cells (Fig. 6B). Consequently, we speculate that GSTO1-1 regulates the TLR4 pathway by the reversible glutathionylation of a key protein.

Overall these findings support our hypothesis that GSTO1-1 is an indispensable upstream modulator of TLR4-mediated responses and is necessary for the maintenance of the metabolic and redox re-profiling of LPS-activated macrophages.

MATERIALS AND METHODS

Materials

Unless otherwise indicated, all chemicals were purchased from Sigma-Aldrich (St. Louis, MO). LPS (*Escherichia coli* O111:B4) was purchased from Invitrogen. The primers used in this study were purchased from Integrated DNA Technology (supplementary material Table S1). Antibodies were purchased from Cell Signaling Technology (Danvers, MA).

The GSTO1-1 inhibitor ML175 {N-[3-(N-(2-chloroacetyl)-4-nitroanilino) propyl]-2,2,2-trifluoroacetamide} is a hindered α-chloroacetamide (Tsuboi et al., 2010) and was purchased from Vitas-M Laboratory (The Netherlands).

Cell culture

Cells lines were purchased from ATCC and were maintained at 37°C, under 5% CO_2 and in Dulbecco's modified Eagle's medium (DMEM) supplemented with 10% fetal bovine serum. J774.1A murine macrophagic

Journal of Cell Science (2015) 128, 1982-1990 doi:10.1242/jcs.167858

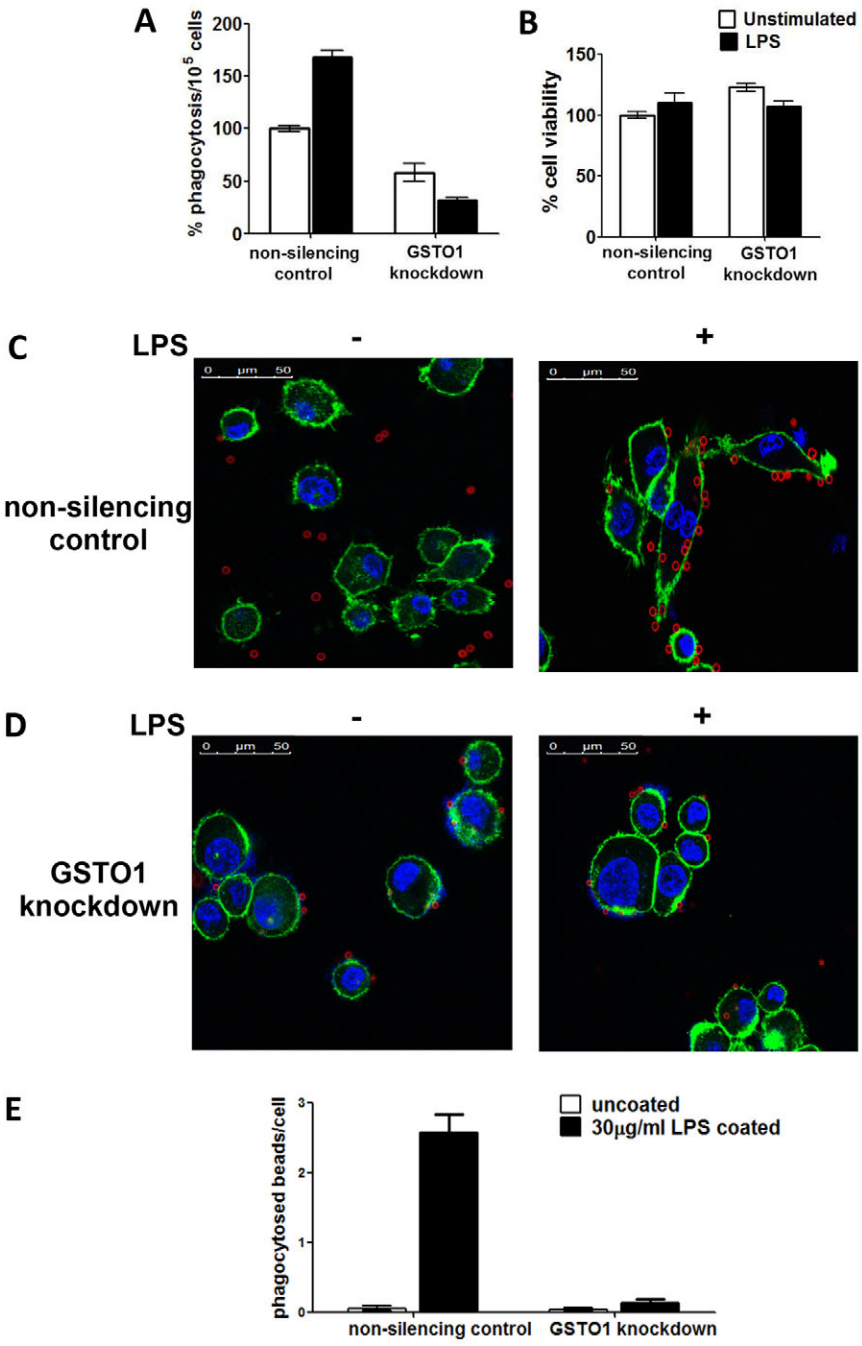

Fig. 5. GSTO1-1 is required for bacterial phagocytosis. (A) Phagocytosis of dead bacteria in GSTO1-1-deficient macrophages was substantially attenuated. (B) Cell viability remained unchanged between the non-silencing control and GSTO1-knockdown cells. (C,D) LPS-stimulated TLR4-dependent phagocytosis was specifically blocked in GSTO1-1-deficient cells. The nucleus is stained with DAPI (blue), the plasma membrane is indicated by actin staining (green) and LPS-coated latex beads are shown in red. (E) The number of beads taken up was evaluated in 200 cells per treatment group from three replicated experiments. All data are shown as the mean±s.e.m. (*n*=3).

cells transfected with a lentiviral plasmid encoding a GSTO1 short hairpin RNA (shRNA) and non-silencing control scrambled shRNA were generated as previously described (Menon et al., 2014). The efficient knockdown of GSTO1-1 by lentiviral shRNA expression is confirmed in Fig. 2B. In all cell culture experiments, LPS was used at a concentration of 10 ng/ml.

Immunoblotting

SDS-PAGE and non-reducing SDS-PAGE were performed as described previously (Laemmli, 1970). Separated proteins were transferred onto nitrocellulose membranes (Towbin et al., 1979) and immunodetected using primary antibodies at a 1:1000 dilution and probed with a goat anti-rabbit IgG horseradish-peroxidase-conjugated secondary antibody (Dako). Chemiluminescence was detected by the ECL Rapid Step chemiluminescence detection system (Calbiochem, Merck, Germany).

Quantification of the cellular glutathione pool

The assay was carried out as described previously (Rahman et al., 2006). For oxidized glutathione, 100 µl of sample or GSSG standards were treated with 10% 2-vinylpyridine (10 µl) for 1 h followed by pH neutralization with 6% triethanolamine (6 µl). For reduced glutathione, 100 µl of sample or GSH standards was assayed directly. Samples were incubated with pre-mixed 5,5′-dithiobis-2-nitrobenzoic acid (DTNB) (0.67 mg/ml) and glutathione reductase (250 U/ml) for 30-s–1-min as per protocol and mixed with NADPH (0.67 mg/ml) and the reaction rate was immediately recorded at 412 nm using a microplate reader.

Real-time RT-PCR

Total RNA was extracted from cells in trizol (Invitrogen) and a Qiagen RNA extraction kit. The extracted RNA was treated with DNase to remove genomic DNA contamination (Ambion DNase kit), and cDNA

Journal of Cell Science (2015) 128, 1982-1990 doi:10.1242/jcs.167858

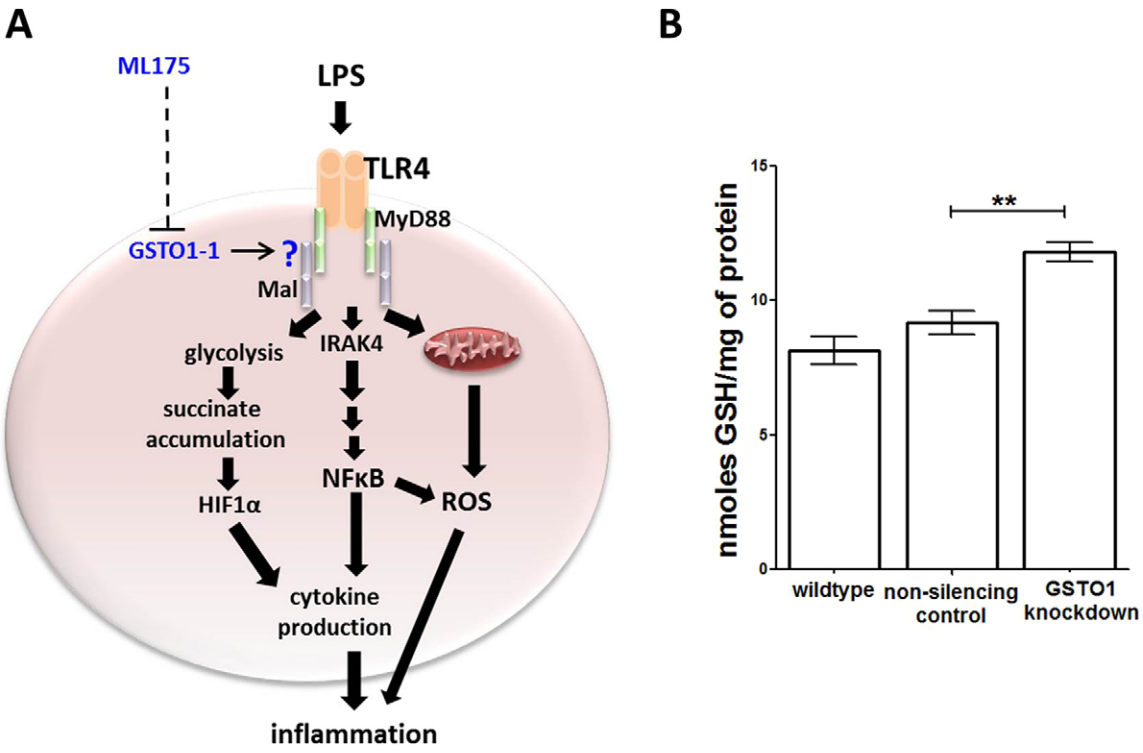

Fig. 6. A scheme proposed for the role of GSTO1-1 in the development of LPS- and TLR4-mediated inflammation. (A) GSTO1-1 deficiency or its inhibition with ML175 blocks the activation of NF-κB, the generation of cytosolic and mitochondrial ROS, and the switch to a glycolytic phenotype characterized by the accumulation of succinate and the stabilization of HIF1α. These effects block pro-inflammatory cytokine production that leads to inflammation. The available evidence suggests that GSTO1-1 targets a protein in the myddsome shown in the red box. (B) GSTO1-1 deficiency leads to a significant (**P<0.01) increase in total protein glutathionylation. Data are shown as the mean±s.e.m. (n=3).

was synthesized by the use of an Invitrogen first-strand cDNA synthesis kit. Real-time PCR was carried out on an ABI 7900HT thermocycler and relative transcript levels were calculated by the ΔΔCt method using GAPDH as an internal control to which all transcripts were normalized. Primer sequences are provided in supplementary material Table S1.

Measuring mitochondrial ROS

Cells were seeded in six-well dishes at a cell density of 5×10^5 cells per well and were treated with LPS as indicated. Cells were washed with PBS and then incubated with MitoSOX and Mitotracker (Life Technologies) for 30 min at 37°C. Cells were washed twice and resuspended in PBS and analysed by fluorescence-activated cell sorting (FACS) analysis. All measurements were normalized against baseline readings from unstained controls and then to untreated controls from each cell type. Data from three independent experiments was analysed using Flowjo FACS analysis software.

Determining mitochondrial membrane potential

Treated or untreated cells (10^5), were resuspended in 1 ml warm PBS. As a positive control, cells were treated with 50 µM Carbonyl cyanide m-chlorophenyl hydrazone (CCCP) for 5 min. Cells were incubated with JC-1 dye (Mitoprobe, Life Technologies) at 37°C, under 5% CO_2 for 30 min according to the manufacturer's instructions. Cells were then washed with PBS and resuspended in 100 µl of PBS and analysed by FACS with an emission wavelength of 488 nm. Data from three independent experiments was analysed using Flowjo FACS analysis software.

Measurement of extracellular lactate levels

Cells were seeded in six-well dishes at a density of 5×10^5 cells per well and treated with LPS as indicated. Briefly, medium was collected at different time points and mixed with 3% perchloric acid. 0.05% Methyl Orange was then added to the samples (final concentration of 0.00083%) and mixed well. The pH of the samples was raised with 1M K_2CO_3 until the solution turned bright yellow. The volume was adjusted to 400 µl and 1/10th of the total volume (40 µl) was then incubated with NAD (1 mM) in a glycine hydrazine buffer (1 M glycine, 0.4 M hydrazine sulphate, 5 mM EDTA and 0.5 M NaOH) and initial absorbance was measured at 340 nm at 37°C. The samples were then mixed with 19.8 U lactate dehydrogenase and absorbance was recorded every 10 min at 340 nm at 37°C. The initial absorbance values were subtracted from the final readings and lactate concentrations were calculated based on the standard curve obtained from standards made from sodium lactate.

Measurement of NADPH and NADP$^+$ levels

Cellular NADPH and NADP levels were estimated by an enzymatic assay (Abnova). Briefly, 10^5 cells were lysed in either NADP or NADPH extraction buffer and heated at 60°C for 5 min. Samples were neutralized with the opposite buffer and centrifuged at 14,000 ***g*** for 10 min to remove all debris. The supernatant was incubated with the reaction buffer (containing MTT, glucose and glucose dehydrogenase) and absorbance was immediately read at 565 nm. The reaction was allowed to progress at room temperature and the final absorbance was measured after 30 min. The initial absorbance values were subtracted from the final readings, and NADPH:NADP ratios were calculated based on NADP standards.

Extracellular flux measurements

For real-time analysis of the bioenergetics profile of activated macrophages (OCR and ECAR), cells were analysed with an XFe-96 Extracellular Flux Analyser (Seahorse Bioscience) as described previously (Freemerman et al., 2014; Haschemi et al., 2012). Cells were seeded at a density of 130,000 cells per well in XFe 96 plates and treated with LPS as indicated. The cells were washed and allowed to recover in XF medium supplemented with 5.5 mM glucose and 1 mM pyruvate for 1 h at 37°C without CO_2. The OCR and ECAR were measured and results were normalized to readings from untreated cells at the respective time points.

GC-MS analysis of metabolites in macrophages

For gas-chromatography–mass-spectrometry (GC-MS) analysis, cells were seeded at a density of 5×10^5 cells per well in six-well dishes and treated with LPS as indicated. Post treatment, cells were lysed in a 1:1 methanol and water solution and derivitized in methoxyamine, HCl in anhydrous pyridine and N-methyl-N-(trimethylsilyl)-trifluoroacetamide. The derivatized samples were analysed by GC-MS with a full scan range of 50–600 *m*/*z* transition (Agilent 7890A, Agilent 5975C MS inert XL EI/CI MSD with triple axis detector, Inc. Santa Clara, CA). Metabolites were screened using AnalyzerPro and identified against the NSIT library. The peak area of Kreb's intermediates succinate and fumarate were normalized to essential amino acids in each sample. All readings were measured in triplicate.

LC-MS/MS analysis of metabolites in macrophages

For liquid-chromatography–tandem-mass-spectrometry (LC-MS/MS) analysis, cells were seeded at a density of 5×10^5 cells per well in six-well dishes and treated with LPS as indicated. Post treatment, cells were washed with PBS and lysed in a 1:1 methanol and water solution and pre-treated as described above for the GC-MS sample preparation. The supernatant was dried using a vacuum concentrator (Savant Speedvac) and resuspended along with the standards in double distilled degassed water. Samples were vortexed and filtered through a 0.45 µm GHP membrane in a Nanosep MF Centrifuge tube (Pall Co., Port Washington, WI) before LC-MS/MS analysis. Sugar phosphates and other metabolic intermediates were analysed using an optimized Agilent 6530 Accurate-Mass Q-TOF LC/MS (Agilent Technologies, Inc. Santa Clara, CA) at the ANU Mass Spectrometry Facility. Samples were subjected to optimized electrospray ionization (ESI) in the Jetstream interface in negative polarity under the following conditions: gas temperature 250°C, drying gas 9 l min^{-1}, nebulizer 25 psig (172.4 kPa), sheath gas temperature 250°C and flow rate of 11 l min^{-1}, capillary voltage 2500 V, fragmentor 145 V, and nozzle voltage 500 V. Mobile phase A consisted of water with 0.1% formic acid and mobile phase B consisted of 90% methanol, 10% water and 0.1% formic acid. Samples were injected onto an Agilent Phonomenex Luna 3U HILIC 200A (50×2 mm, 3 micron) column and analytes were eluted in mobile phase B. The quadrupole-time-of-flight (QTOF) was operated in targeted MS/MS mode using collision-induced dissociation [CID; N2 collision gas supplied at 18 psi (124.1 kPa), *m*/*z* 1.3 isolation window] where the MS extended dynamic range was set from *m*/*z* 100–1000 at three spectra s^{-1}, and MS/MS *m*/*z* 50–1000 at three spectra s^{-1}. Data was extracted and analysed using Agilent Technologies Masshunter software.

Phagocytosis assay

Phagocytosis of fluorescently labelled dead *E. coli* (strain K-12) was measured as per manufacturer's instructions (Vybrant phagocytosis kit, Life Technologies). J774.1A cells were seeded in 96-well plates at a density of 10^5 cells per well and allowed to adhere for 2 h at 37°C, 5% CO_2. Medium was removed and the cells were incubated in the fluorescent bioparticle suspension for 2 h. The supernatant was then removed and Trypan Blue was added to each well at a final concentration of 250 µg/ml and allowed to sit for 1 min. The wells were washed and fluorescence was measured at an excitation and emission wavelength of 480 and 520 nm, respectively, using a plate reader (Fluostar Optima). Net phagocytosis of GSTO1-1 knockdown cells was determined by subtracting the average fluorescence of media-only negative control wells and normalizing to the average fluorescence of the non-silencing control J774.1A macrophages. The cells were then lysed in 1% SDS and cell viability was determined by measuring absorbance of Trypan Blue at 590 nm (Uliasz and Hewett, 2000).

Latex bead phagocytosis assay

Yellow–orange 3-µm Fluoresbrite carboxy latex microparticles (Polysciences) were incubated with 30 µg/ml LPS overnight at 4°C in PBS. Beads were then washed thoroughly in PBS to remove unbound LPS. Cells cultured overnight on coverslips in 12-well plates were incubated on ice for 10 min. LPS-coated and uncoated (control) latex beads were added to the cells and allowed to settle on the cells for 10 min prior to incubation in warm culture medium at 37°C for indicated time periods. Cells were fixed with 3.7% paraformaldehyde for 15 min at room temperature, permeabilized with 0.1% Triton X-100 and 0.2% BSA and stained with phalloidin–FITC (Sigma) as per the manufacturer's instructions. The intracellular uptake of the beads was visualized by confocal microscopy (Leica SP5). Serial *z*-sections were recorded to confirm intracellular localization of the beads. The number of beads taken up was assessed in 200 cells per treatment group across 30 cells per coverslip.

Statistical analysis

Data were expressed as the mean±s.e.m. and analysed using Prism 4 (Graphpad software Inc.). Statistical significance was calculated by standard Student's *t*-tests. All experiments were performed in triplicate unless otherwise stated. Statistical significance was shown as $*P\leq0.05$, $**P<0.01$ and $***P<0.001$.

Acknowledgements

We thank Dr Thy Truong (ANU Mass spectrometry Facility) for her assistance with the mass spectrometry experiments.

Competing interests

The authors declare no competing or financial interests.

Author contributions

D.M. participated in the planning and undertook most of the experiments. D.M. was also involved in the analysis and interpretation of the data and the preparation of the manuscript. R.C. contributed to the planning of the experiments and generated the knockdown cell line. L.A.J.O. contributed to the project planning, the interpretation of the results and provided discussion during the preparation of the manuscript. P.G.B. supervised the project, helped interpret the results and played a significant role in the preparation of the manuscript.

Funding

This work was supported by a grant from the Gretel and Gordon Bootes Medical Research Foundation to D.M. and P.G.B.

Supplementary material

Supplementary material available online at
http://jcs.biologists.org/lookup/suppl/doi:10.1242/jcs.167858/-/DC1

References

Allen, M., Zou, F., Chai, H. S., Younkin, C. S., Miles, R., Nair, A. A., Crook, J. E., Pankratz, V. S., Carrasquillo, M. M., Rowley, C. N. et al. (2012). Glutathione S-transferase omega genes in Alzheimer and Parkinson disease risk, age-at-diagnosis and brain gene expression: an association study with mechanistic implications. *Mol. Neurodegener.* **7**, 13.

Anathy, V., Roberson, E. C., Guala, A. S., Godburn, K. E., Budd, R. C. and Janssen-Heininger, Y. M. W. (2012). Redox-based regulation of apoptosis: S-glutathionylation as a regulatory mechanism to control cell death. *Antioxid. Redox Signal.* **16**, 496-505.

Chen, C., Chen, Y. H. and Lin, W. W. (1999). Involvement of p38 mitogen-activated protein kinase in lipopolysaccharide-induced iNOS and COX-2 expression in J774 macrophages. *Immunology* **97**, 124-129.

Cooper, A. J. L., Pinto, J. T. and Callery, P. S. (2011). Reversible and irreversible protein glutathionylation: biological and clinical aspects. *Expert Opin. Drug Metab. Toxicol.* **7**, 891-910.

D'Acquisto, F., Iuvone, T., Rombolà, L., Sautebin, L., Di Rosa, M. and Carnuccio, R. (1997). Involvement of NF-kappaB in the regulation of cyclooxygenase-2 protein expression in LPS-stimulated J774 macrophages. *FEBS Lett.* **418**, 175-178.

Dalle-Donne, I., Rossi, R., Colombo, G., Giustarini, D. and Milzani, A. (2009). Protein S-glutathionylation: a regulatory device from bacteria to humans. *Trends Biochem. Sci.* **34**, 85-96.

Doyle, S. L. and O'Neill, L. A. (2006). Toll-like receptors: from the discovery of NFkappaB to new insights into transcriptional regulations in innate immunity. *Biochem. Pharmacol.* **72**, 1102-1113.

Escobar-Garcia, D. M., Del Razo, L. M., Sanchez-Pena, L. C., Mandeville, P. B., Lopez-Campos, C. and Escudero-Lourdes, C. (2012). Association of glutathione S-transferase Omega 1-1 polymorphisms (A140D and E208K) with the expression of interleukin-8 (IL-8), transforming growth factor beta (TGF-beta), and apoptotic protease-activating factor 1 (Apaf-1) in humans chronically exposed to arsenic in drinking water. *Arch. Toxicol.* **86**, 857-868.

Freemerman, A. J., Johnson, A. R., Sacks, G. N., Milner, J. J., Kirk, E. L., Troester, M. A., Macintyre, A. N., Goraksha-Hicks, P., Rathmell, J. C. and Makowski, L. (2014). Metabolic reprogramming of macrophages: glucose transporter 1 (GLUT1)-

mediated glucose metabolism drives a proinflammatory phenotype. *J. Biol. Chem.* **289**, 7884-7896.

Gauss, K. A., Nelson-Overton, L. K., Siemsen, D. W., Gao, Y., DeLeo, F. R. and Quinn, M. T. (2007). Role of NF-kappaB in transcriptional regulation of the phagocyte NADPH oxidase by tumor necrosis factor-α. *J. Leukoc. Biol.* **82**, 729-741.

Gill, R., Tsung, A. and Billiar, T. (2010). Linking oxidative stress to inflammation: toll-like receptors. *Free Radic. Biol. Med.* **48**, 1121-1132.

Harju, T. H., Peltoniemi, M. J., Rytilä, P. H., Soini, Y., Salmenkivi, K. M., Board, P. G., Ruddock, L. W. and Kinnula, V. L. (2007). Glutathione S-transferase omega in the lung and sputum supernatants of COPD patients. *Respir. Res.* **8**, 48.

Haschemi, A., Kosma, P., Gille, L., Evans, C. R., Burant, C. F., Starkl, P., Knapp, B., Haas, R., Schmid, J. A., Jandl, C. et al. (2012). The sedoheptulose kinase CARKL directs macrophage polarization through control of glucose metabolism. *Cell Metab.* **15**, 813-826.

Kölsch, H., Linnebank, M., Lütjohann, D., Jessen, F., Wüllner, U., Harbrecht, U., Thelen, K. M., Kreis, M., Hentschel, F., Schulz, A. et al. (2004). Polymorphisms in glutathione S-transferase omega-1 and AD, vascular dementia, and stroke. *Neurology* **63**, 2255-2260.

Laemmli, U. K. (1970). Cleavage of structural proteins during the assembly of the head of bacteriophage T4. *Nature* **227**, 680-685.

Li, Y. J., Oliveira, S. A., Xu, P., Martin, E. R., Stenger, J. E., Scherzer, C. R., Hauser, M. A., Scott, W. K., Small, G. W., Nance, M. A. et al. (2003). Glutathione S-transferase omega-1 modifies age-at-onset of Alzheimer disease and Parkinson disease. *Hum. Mol. Genet.* **12**, 3259-3267.

Lim, S. Y., Raftery, M. J., Goyette, J. and Geczy, C. L. (2010). S-glutathionylation regulates inflammatory activities of S100A9. *J. Biol. Chem.* **285**, 14377-14388.

Maitra, U., Singh, N., Gan, L., Ringwood, L. and Li, L. (2009). IRAK-1 contributes to lipopolysaccharide-induced reactive oxygen species generation in macrophages by inducing NOX-1 transcription and Rac1 activation and suppressing the expression of antioxidative enzymes. *J. Biol. Chem.* **284**, 35403-35411.

Matsuzawa, A., Saegusa, K., Noguchi, T., Sadamitsu, C., Nishitoh, H., Nagai, S., Koyasu, S., Matsumoto, K., Takeda, K. and Ichijo, H. (2005). ROS-dependent activation of the TRAF6-ASK1-p38 pathway is selectively required for TLR4-mediated innate immunity. *Nat. Immunol.* **6**, 587-592.

Meissner, F., Molawi, K. and Zychlinsky, A. (2008). Superoxide dismutase 1 regulates caspase-1 and endotoxic shock. *Nat. Immunol.* **9**, 866-872.

Menon, D. and Board, P. G. (2013). A role for glutathione transferase Omega 1 (GSTO1-1) in the glutathionylation cycle. *J. Biol. Chem.* **288**, 25769-25779.

Menon, D., Coll, R., O'Neill, L. A. J. and Board, P. G. (2014). Glutathione transferase omega 1 is required for the lipopolysaccharide-stimulated induction of NADPH oxidase 1 and the production of reactive oxygen species in macrophages. *Free Radic. Biol. Med.* **73**, 318-327.

Mo, C., Wang, L., Zhang, J., Numazawa, S., Tang, H., Tang, X., Han, X., Li, J., Yang, M., Wang, Z. et al. (2014). The crosstalk between Nrf2 and AMPK signal pathways is important for the anti-inflammatory effect of berberine in LPS-stimulated macrophages and endotoxin-shocked mice. *Antioxid. Redox Signal.* **20**, 574-588.

Piacentini, S., Polimanti, R., Squitti, R., Mariani, S., Migliore, S., Vernieri, F., Rossini, P. M., Manfellotto, D. and Fuciarelli, M. (2012). GSTO1*E155del polymorphism associated with increased risk for late-onset Alzheimer's disease: association hypothesis for an uncommon genetic variant. *Neurosci. Lett.* **506**, 203-207.

Poltorak, A., He, X., Smirnova, I., Liu, M.-Y., Van Huffel, C., Du, X., Birdwell, D., Alejos, E., Silva, M., Galanos, C. et al. (1998). Defective LPS signaling in C3H/HeJ and C57BL/10ScCr mice: mutations in Tlr4 gene. *Science* **282**, 2085-2088.

Rahman, I., Kode, A. and Biswas, S. K. (2006). Assay for quantitative determination of glutathione and glutathione disulfide levels using enzymatic recycling method. *Nat. Protoc.* **1**, 3159-3165.

Raso, G. M., Meli, R., Di Carlo, G., Pacilio, M. and Di Carlo, R. (2001). Inhibition of inducible nitric oxide synthase and cyclooxygenase-2 expression by flavonoids in macrophage J774A.1. *Life Sci.* **68**, 921-931.

Stoll, L. L., Denning, G. M. and Weintraub, N. L. (2006). Endotoxin, TLR4 signaling and vascular inflammation: potential therapeutic targets in cardiovascular disease. *Curr. Pharm. Des.* **12**, 4229-4245.

Tannahill, G. M., Curtis, A. M., Adamik, J., Palsson-McDermott, E. M., McGettrick, A. F., Goel, G., Frezza, C., Bernard, N. J., Kelly, B., Foley, N. H. et al. (2013). Succinate is an inflammatory signal that induces IL-1β through HIF-1α. *Nature* **496**, 238-242.

Thimmulappa, R. K., Scollick, C., Traore, K., Yates, M., Trush, M. A., Liby, K. T., Sporn, M. B., Yamamoto, M., Kensler, T. W. and Biswal, S. (2006). Nrf2-dependent protection from LPS induced inflammatory response and mortality by CDDO-Imidazolide. *Biochem. Biophys. Res. Commun.* **351**, 883-889.

Towbin, H., Staehelin, T. and Gordon, J. (1979). Electrophoretic transfer of proteins from polyacrylamide gels to nitrocellulose sheets: procedure and some applications. *Proc. Natl. Acad. Sci. USA* **76**, 4350-4354.

Tsuboi, K., Bachovchin, D. A., Speers, A. E., Brown, S. J., Spicer, T., Fernandez-Vega, V., Ferguson, J., Cravatt, B. F., Hodder, P. and Rosen, H. (2010). Optimization and characterization of an inhibitor for glutathione S-tranferase omega 1 (GSTO1). In *Probe Reports from the NIH Molecular Libraries Program* (ed. NCBI (US)). Bethesda, MD: NCBI.

Uliasz, T. F. and Hewett, S. J. (2000). A microtiter trypan blue absorbance assay for the quantitative determination of excitotoxic neuronal injury in cell culture. *J. Neurosci. Methods* **100**, 157-163.

Wadleigh, D. J., Reddy, S. T., Kopp, E., Ghosh, S. and Herschman, H. R. (2000). Transcriptional activation of the cyclooxygenase-2 gene in endotoxin-treated RAW 264.7 macrophages. *J. Biol. Chem.* **275**, 6259-6266.

West, A. P., Brodsky, I. E., Rahner, C., Woo, D. K., Erdjument-Bromage, H., Tempst, P., Walsh, M. C., Choi, Y., Shadel, G. S. and Ghosh, S. (2011). TLR signalling augments macrophage bactericidal activity through mitochondrial ROS. *Nature* **472**, 476-480.

Zhang, G. and Ghosh, S. (2001). Toll-like receptor-mediated NF-kappaB activation: a phylogenetically conserved paradigm in innate immunity. *J. Clin. Invest.* **107**, 13-19.

Zhou, R., Tardivel, A., Thorens, B., Choi, I. and Tschopp, J. (2010). Thioredoxin-interacting protein links oxidative stress to inflammasome activation. *Nat. Immunol.* **11**, 136-140.